1.1 REMOTE SENSING OF CHEMICAL SPECIES IN THE ATMOSPHERE

C. Russell Philbrick[1,2,3], David M. Brown[1], Adam H. Willitsford[1], Perry S. Edwards[1], Andrea M. Wyant[1], Zhiwen Z. Liu[1], C. Todd Chadwick[2], and Hans Hallen[2]

[1]Department of Electrical Engineering, Penn State University, University Park, PA 16802,
[2]Physics Department and [3]Marine, Earth, and Atmospheric Sciences Department,
North Carolina State University, Raleigh NC 27606-8202
Email: crp3@psu.edu, (919) 515-7828

***Abstract* – Laser remote sensing techniques now provide capabilities for measuring the primary natural atmospheric species and can also be used to detect several of the air pollutants and precursors emitted into the atmosphere or deposited onto surfaces. In recent years, interests in developing sensors capable of detecting lower concentration levels of various species has increased for applications in air pollution monitoring, and for warnings of the presence of hazardous chemicals. Our long term efforts have focused on developing and using various applications of Raman and DIAL lidar techniques to measure atmospheric species, pollutants and aerosols. Our recent efforts are focused on developing the capabilities of multi-wavelength differential absorption lidar techniques extended to infrared wavelengths, and resonance-Raman scattering at ultraviolet wavelengths. Broadband supercontinuum lasers used as transmitter sources provide a new capability for measuring chemical species while performing multi-wavelength differential absorption lidar (DIAL) analysis. This technique opens the opportunity of applying well-developed spectroscopy techniques and hyper-spectral remote sensing for measuring the concentrations of molecular species. Resonance-Raman scattering techniques using ultraviolet wavelengths are being developed to extend our detection to small concentration levels of certain chemical species. These two new techniques advance our capability to measure the chemical species. Recent measurement results, simulations, and calculations are used to describe our current capabilities, and indicate future directions for these applications in laser remote sensing.**

I. INTRODUCTION

The goal of this paper is to summarize our current capabilities and describe new approaches being development for detecting low concentrations of chemical species using optical absorption and scattering processes. The detection of chemical species depends upon several factors: (1) sufficient signal strength, (2) distinctive features in the detected signal, and (3) uniqueness of the signal features for the chemical species of interest, when compared relative to the backgrounds of interfering signals.

II. PROCESSES FOR SPECIES MEASUREMENTS

Each molecule making up a chemical sample is composed of a unique combination of the elements held together with several types of bonds of different strengths. The different masses and bonds lead to the unique set of quantized energy levels associated with vibrational, rotational, stretching and bending modes of the molecules; thereby leading to unique identification of a chemical species. We can observe the uniqueness of essentially every chemical species by observing the infrared absorption spectra, or the Raman scattering intensity within the region of the spectrum, 0 - 4200 cm^{-1}, which corresponds to absorption spectrum wavelengths from about 25 to 2.4 μm. This spectral region (see Fig. 1) contains many observable absorption features associated with the energies of the vibrational, rotational, bending, stretching, and other oscillatory modes of the molecules in the optical spectrum; the most energetic being the vibrational mode of the H_2 molecule at 4150 cm^{-1} (~2.5 μm). At higher frequency, shorter wavelengths, the harmonics (over-tones) and more energetic electronic activity of molecular and atomic bonds are observed for several molecules. The spectra features of molecules with hydrogen bonded to carbon, nitrogen, and oxygen are typically observed in the region between 2.5 and 5 μm. In most cases, spectral features are well identified with the quantized energy states of oscillatory motions of molecules. In some of the more complicated long chain molecules, these features are identified with the sub-group clusters of molecules that attach in chain-like fashion. In even more complicated molecules or cell structures, only a few of the primary spectral features of cluster molecules and bond types may be distinctly identified in the absorption spectra.

The second major way of identifying a chemical species is by examining the scattered optical radiation, or Raman scattering spectrum. Molecular bonds, with any small asymmetry in the charge distribution of bound or shared electrons, can be forced into oscillation by the presence of an oscillatory electric field. Thus, any passing photon has the opportunity to scatter from a molecule and force the oscillation of the many different energetic modes in the molecule. The scattered photon can leave with less energy by a precise amount (red-shifted), which refers to the Stokes component, and the energy difference corresponds to the energy gained by the molecule. If the molecule is already residing in a higher energy state, then the scattered photon may acquire additional energy, and the spectrum of the scattered radiation is referred to as anti-Stokes Raman scatter.

Additional optical techniques for chemical species analysis include Laser Inducted Breakdown Spectra (LIBS) and fluorescent emission. The LIBS technique uses a focused laser beam to rupture the molecular structure with intense electric fields. In the process, a large number of excited states of the atomic components are created; these emissions often permit identification of the likely parent species. Fluorescent emissions are excited by optical radiation, most often in the blue and ultraviolet region, and the presence of molecular types and compounds can often be detected; thereby allowing a technique with more specificity to identify it. These last two techniques will not be elaborated on further in this report.

Infrared optical absorption and Raman scatter intensity measurements provide complementary pictures of the energy states of a molecule and permit unique identifications for most species, based upon the dynamical resonances that exist within a molecule. Often the same energy state will appear as both infrared active and Raman active; while some of the energy states are only observed in either the infrared absorption or in the Raman scatter spectra of a molecule; both techniques provide spectral "fingerprints" that are quite specific for identifying molecules.

When the molecule is in a liquid form or smeared as a compound with other materials, the response of the energy states to the impinging radiation is altered in intensity, and is typically shifted by the stiffening of the bonds between the atoms. However, the spectral features are usually recognized to identify which chemical species and what concentrations are present.

A. Infrared Absorption

Molecular vibration is **infrared active** if the molecule's normal dipole moment is modulated. The impinging radiation field must be near the same frequency as an oscillation resonance of the electric dipole moment if the radiation is to be absorbed. The resonance occurs at an energy corresponding to a vibrational, rotational, stretching, bending, rocking, wagging, twisting, or other oscillatory energy states of a molecule. The infrared spectrum can be considered to extend from 1000 μm (10 cm^{-1}) to 0.7 μm (14,000 cm^{-1}); the sub-ranges are often referred to as near-IR (beginning 0.7 μm, 14,000 cm^{-1}), mid-IR (beginning 2.4 μm, 4,200 cm^{-1}), long-IR (beginning 8 μm, 1250 cm^{-1}), and far-IR (beginning 25 μm, 400 cm^{-1}). Most of the absorption features that are used for optical spectra identification are found in the region between 2.5 and 25 μm (4,000 to 400 cm^{-1}).

The spectrum of the absorption of optical radiation by the molecules of the background atmosphere is shown in Fig. 1. Here the atmospheric column absorption from space to the Earth's surface is shown using the MODTRAN™ atmospheric model [1]. The visible region between 0.4 and 0.7 μm is relatively free of absorption and scattering along the vertical path through the atmosphere, and primarily experiences extinction from scattering by molecules (principally nitrogen and oxygen), or by aerosols. The ultraviolet region, between 0.4 μm to 0.2 μm, exhibits rapidly decreasing transmission at shorter wavelengths due to strongly increasing molecular scattering, and that gives way to even stronger UV absorption by ozone. Eventually below 0.2 μm, the radiation is absorbed and dissociates the O_2 molecule, and at even shorter wavelengths, the radiation dissociates and ionizes all of the molecular species with essentially complete absorption of any EUV (extreme ultraviolet) radiation. The infrared region between 0.7 and 2.5 μm contains the harmonic overtones of the strongly absorbing primary species. The region from 2.5 to 25 μm contains the spectral signatures that are used to identify and quantify chemical species using optical absorption techniques, while Raman scatter measurements are generally carried out using visible and ultraviolet radiation because of the larger cross-section ($\sigma \propto 1/\lambda^4$).

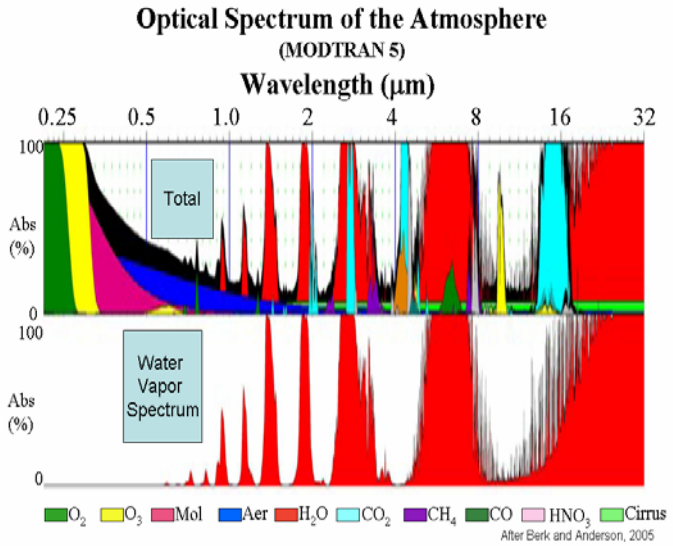

Figure 1. The vertical path integrated optical absorption between space and ground as calculated using the MODTRAN™ model for optical propagation [1].

B. Raman Scatter

A molecule is **Raman active** if a dipole is induced by the action of the electric field of a scattering photon, which forces a relative motion between the electrons and the nuclei. The induced dipole moment is proportional to the radiation intensity's electric field strength and the polarizability of the molecule. Some of the same vibrational and other oscillatory energy states observed in infrared absorption, when the molecule has an electric dipole moment, are also observed as same energy shifts in scattered Raman signals, when a dipole moment is induced. Additional spectral features found in the Raman spectra complement the process of identification. In the case of Raman scattering, rather than signals located in the 2.5 to 25 μm wavelength region, the scattered signals are located at the wavelength corresponding to the energy difference from the excitation wavelength. The vibrational energy states are most useful for identifying and quantifying the molecule because of their unique character determined by the molecular moment of inertia and its bond strengths. The possibility of using the Raman scattering for lidar measurements was described in some detail in early papers by Inaba and his colleagues in the 1970's [2-4]. The vibrational

energy shifts are shown in Fig. 2 for several common species of interest [2]. The Nd:YAG laser has become the primary transmitter used for Raman lidar investigations during the past two decades. It has the advantage of providing a high output power, and the 1.064 μm fundamental wavelength can be used to generate 2nd, 3rd, and 4th harmonic outputs in the visible and ultraviolet wavelengths. In Fig. 2 the wavelengths of Raman scattered signals from N_2, O_2, and H_2O molecules are indicated for these laser lines.

C. Scattering Processes

The scattering of optical radiation by molecular species provides several different types of signals for detecting various chemical species and measuring concentrations and distributions. In Fig. 3, energy level diagrams are used to represent the several scattering processes that can be used to investigate chemical species.

Fig. 3 shows the several processes that occur as optical wavelengths interact with molecules. First, the infrared absorption process is depicted as absorbed energy raises a molecule to a higher vibrational level. The energies typically correspond to wavelengths between 2.5 and 25 μm. Many other types of oscillatory motions, which correspond to quantized energies of rotation, bending, etc., also can be observed as absorption features. The processes of scattering result in Rayleigh scatter, Mie scatter, and Raman scatter signals. In each of these cases, the interaction may be viewed as the molecule existing in a 'virtual energy' state at the instant the photon energy packet interacts with the molecule or aerosol particle. In most of the cases, the particle returns to the ground state and gives back the same energy photon that was incident – possibly shifted slightly by the Doppler velocity of the ensemble of scattering particles. The cross-sections for the several interactions are indicated in Table I. The cross-section increases for molecules as the probe wavelength decreases to smaller values ($\sigma \propto 1/\lambda^4$), and it increases as the aerosol size increases ($\sigma \propto a^6$).

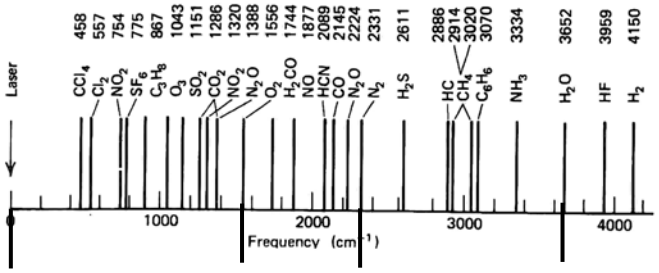

[after Inaba and Kobayasi, 1972]

Figure 2. The frequency shifts of several common molecules are indicated. These represent the energy difference for Stokes and anti-Stokes shifts toward the red and blue direction from the excitation source. The wavelengths expected for excitation by an Nd:YAG laser second, third and fourth harmonics are indicated for the N_2, O_2, and H_2O molecules [2].

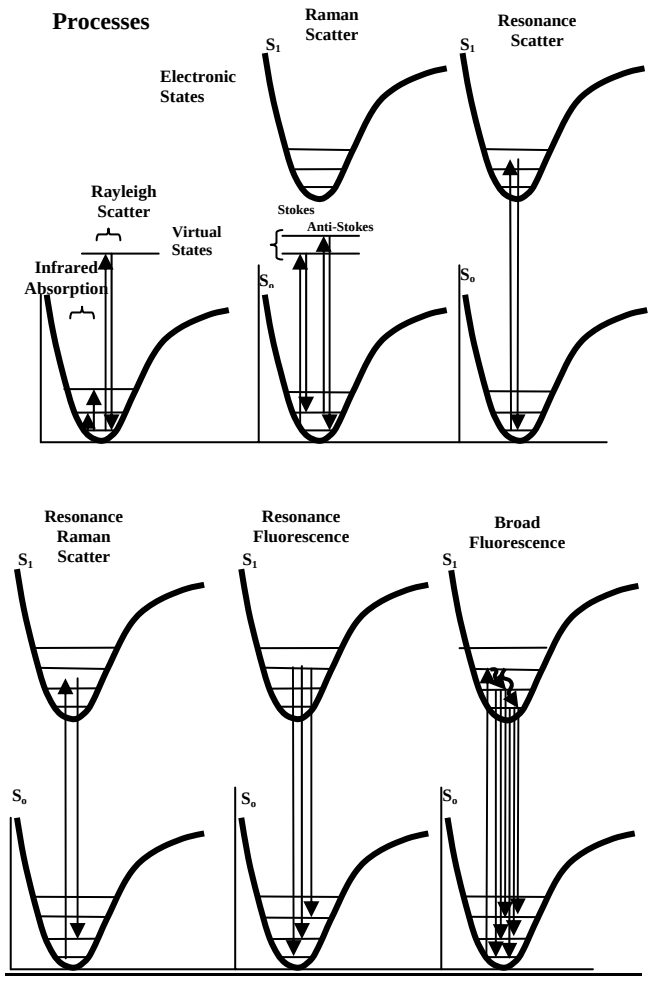

Figure 3. The several processes involving the interactions of incident optical radiation on molecules; processes include infrared absorption, Rayleigh scattering, Raman scattering, and resonance scattering processes.

Table I. Approximate Cross-sections

Process	Type	Cross section (cm2/sr)	Use
Scattering	**Rayleigh**	**$\sim 10^{-26}$**	**Atmosphere T, r**
	Mie	**10^{-26}-10^{-8}**	**Aerosols, particles a, n, r**
	Raman		
	Non-resonance	**10^{-30}-10^{-28}**	**Molecules T, [Ni], a**
	Resonance	**10^{-28}-10^{-20}**	**[N_i]**
Absorption	**DIAL**	**10^{-24}-10^{-20}**	**[N_i]**
	DAS	**~(DIAL) x 10^4**	**N_i (path integrated)**
Emission	**Fluorescence**	**10^{-26}-10^{-20}**	**Species detection ~N_i (quenching)**

As the molecule relaxes from the 'virtual energy condition,' it may return to a different energy state (Stokes or anti-Stokes), the scattered photon will be red-shifted or blue-shifted from the initially incident one. Because the allowed final energy states correspond to precise and discrete changes associated with the vibrational energy levels, it is then

possible to identify the species and measure their concentrations using Raman scatter signals. Cross sections for Raman scatter at the Stokes (red-shifted) wavelengths are typically 10^3 smaller than the Rayleigh scatter at the central Cabannas line. In some cases, significant increases in the Raman cross-sections, see Table I, can be gained when the photon energy is near an electronic state energy. The added resonant response of the electronic state from the photon's electric field results in much higher Raman scatter efficiency. When the photon energy is sufficient to directly excite the electronic states, fluorescence emission is often observed.

D. Raman Lidar Measurements

The Raman scatter signals can be effectively used in lidar applications to measure species concentrations. Fig. 4 shows an example of water vapor measurements using the ratio of water vapor to nitrogen Raman signals [5-7].

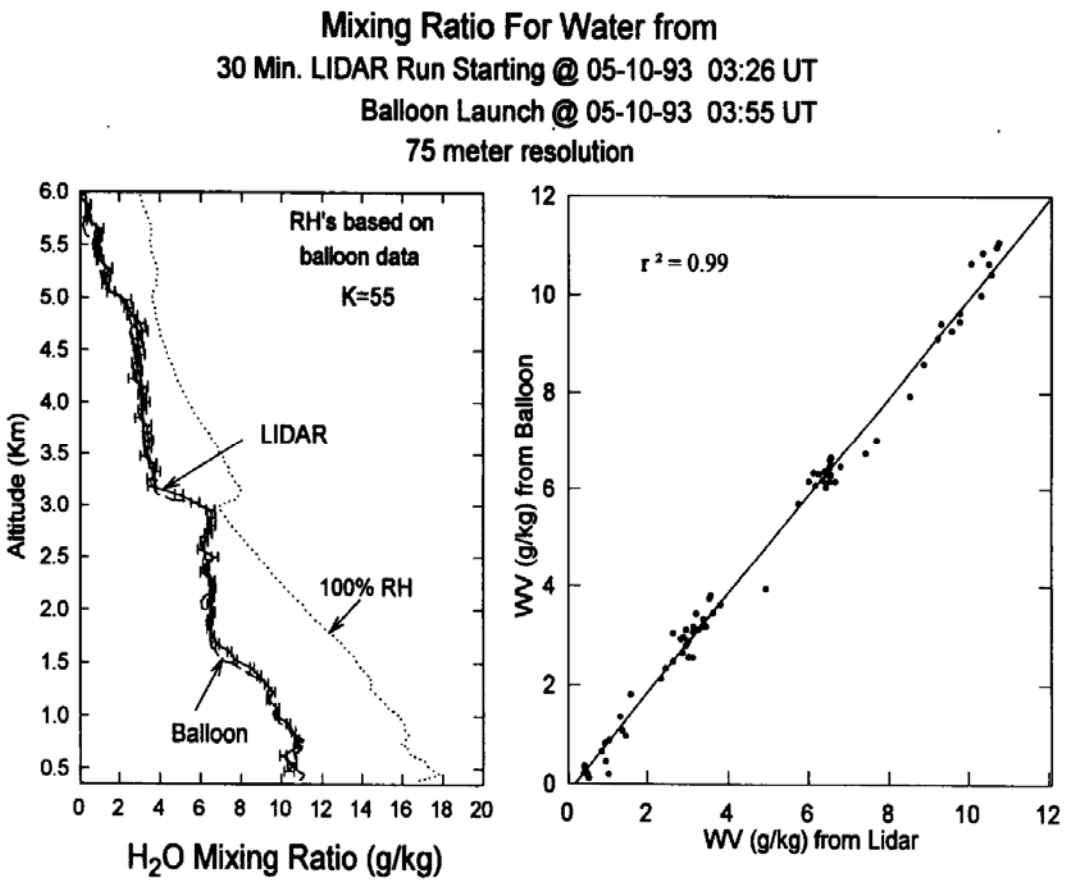

Figure 4. The water vapor specific humidity profiles measured with the PSU LAMP lidar system are compared with simultaneous Rawinsonde balloon release from Pt. Mugu CA [6].

The measurements of many atmospheric species can be obtained from the Raman scattered signal of the selected species by forming a ratio to the nitrogen signal. Since laboratory measurements have provided the accurate Raman cross-sections for most chemical species, the ratio to nitrogen provides accurate profiles of selected species concentrations. By taking the ratio to the known nitrogen density, the density profile of the selected species is also known, and most of the instrument calibration values and system performance unknowns cancel out during the calculation of the species density profile.

Another example of a minor species that can be measured using Raman scatter is shown in Fig. 5. The ozone profile is measured by using the ratio of the O_2 to N_2 signals from the 266 nm 4th harmonic of the Nd:YAG laser [7, 8]. The oxygen to nitrogen ratio should be constant in time, and throughout the lower atmosphere, to within about $1{:}10^5$.

The two Raman scatter wavelengths, 277.6 nm (O_2) and 283.3 nm (N_2), occur on the steep slope of the Hartley absorption band of ozone, and thus any change in their relative signal ratio as a function of altitude is due to absorption. A survey shows that ozone is the species with a differential absorption for these two wavelengths. Since accurate laboratory measured cross-sections for ozone are available, this technique provides a very accurate and robust measurement of ozone. The only significant error is the signal/noise relationship, thus the measurements can be improved with higher power lasers or larger receiving telescopes. The lidar profile of ozone is compared in Fig. 5 with a simultaneously measured aircraft profile [9]. The large scatter differences in the data above 2 km are due to the limited lidar signals from longer ranges. The technique has been used for several intensive investigations of air quality [10-12].

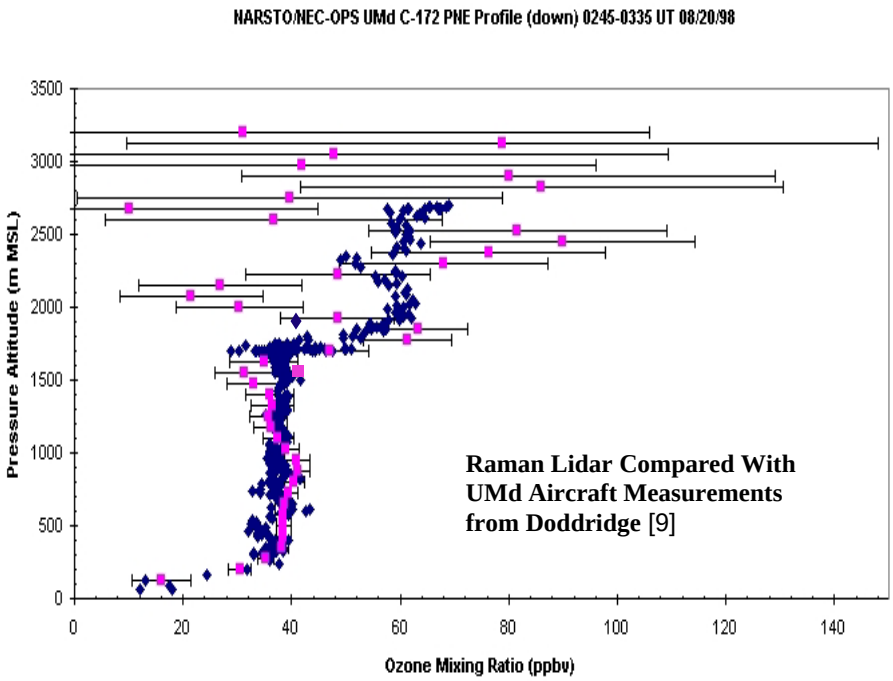

Figure 5. LAPS Raman lidar measurements of ozone are compared with simultaneous aircraft data [9].

The Raman lidar measurements of water vapor, and temperature from the rotational Raman scattered signals allows us to calculate the relative humidity and the RF refractivity. The relative humidity values are straight forward to calculate from Raman lidar measurements and are important for detecting the regions where sub-visual clouds begin to form [10-12]. The RF refractivity measurements are important for radar interpretation because of the ducting effecting on beam propagation [13-15]. Fig. 6 shows the analysis of the meteorological influences upon the RF refraction and demonstrates that it is the water vapor gradients that cause the largest effect on radar interpretation. Calculations of the attenuation of a radar beam shows bending of the radar beam with the signal ducts bent over the horizon [13].

E. Differential Absorption Lidar (DIAL)

During the past four years, an effort by ITT Space Systems, supported by Penn State researchers, has resulted in development of a three wavelength mid-IR DIAL system that is capable of measuring natural gas pipeline leaks as an aircraft flies over the surveyed pipeline location [15-17]. The lidar is deployed in an aircraft so that long segments of pipeline can be rapidly surveyed. Fig. 7 shows an example of a pipeline leak detection superimposed onto an image. In this example, the upper picture shows the geospatial location of the laser spot locations on the ground image, with the threshold detection triggers indicated, and the lower picture shows the regions of high concentrations of methane leaking from a buried pipeline. This sensor has greatly advanced the capability for remote detection of trace concentrations of gases. The ANGEL system can survey hundreds of miles of pipeline in one day compared to earlier practice of sending a man in a jeep to survey 20 miles in a day. The instrument can detect a leak with a single set of three near simultaneous laser shots, and the repetition rate is near 1 kHz as the aircraft follows a GPS determined pipeline route. Developing this system has been a major task; however, it has become the first commercial operational DIAL lidar system.

F. Supercontinuum Laser for SPR-DIAL

The broad spectrum that can be achieved using a femtosecond laser pulse into a photonic crystal fiber opens a new opportunity for measurement and analysis of many wavelengths as DIAL pairs at the same time [18-20]. An example of the type of analysis that can be accomplished is indicated in Fig. 8. This figure shows the spectral features of water measured using the supercontinuum laser as transmitter for lidar, and is compared with the MODTRAN model calculated at the resolution of the spectrometer used for the detector in these experiments. Spectral Pattern Recognition – Differential Absorption Lidar (SPR-DIAL) provides many simultaneous wavelengths that can be used to advantage in discriminating against interfering signals. The technique of using an extensive set of spectral features for a DIAL type analysis, as opposed to just using a paired on-line to off-line ratio to find the concentration has a major advantage in reducing measurement errors. The technique is being used to study atmospheric paths over distances of hundreds of meters at this time, and we expect that paths of kilometer lengths will be measured in the near future. The systems that have been used during the past two years have operated in the region from the ultraviolet (~350 nm) through the near-IR (~1.7 μm), but the next generation sensor will extend the measurements into the mid-IR (1.5-5 μm).

$N = (n - 1) \times 10^6 = 77.6\ P/T + 3.73 \times 10^5\ e/T^2$

$e\ (mb) = (r\ P)/(r + 621.97)$

P - surface pressure r - specific humidity T - temperature

T(K) ~ 295 K P(mb) ~ 1000 mb r ~ 7 g/kg N ~ 310

$\partial N/\partial r \sim 6.7 \quad \partial N/\partial T \sim -1.35 \quad \partial N/\partial P \sim 0.35$

$dN/dz = 6.7\ dr/dz - 1.35\ dT/dz + 0.35\ dP/dz$

Gradients in water vapor are most important in determining RF ducting conditions.

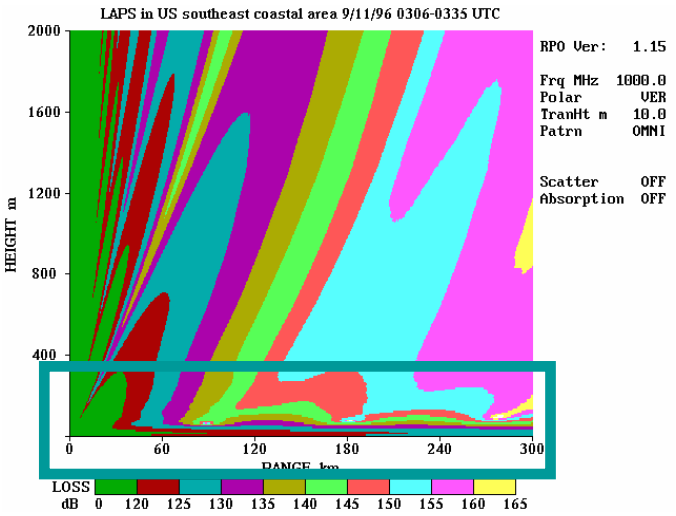

Figure 6. The equations above are used to calculate RF refraction and examine the water vapor influence, and the RPO (Refractive Propagation Optical) model is used with lidar data to show RF ducting effects during shipboard tests [13-15].

F. Resonance Raman and Fluorescence

In collaboration with colleagues from North Carolina State University, the properties of resonance Raman scattering are being investigated. The topic is pursued with the intent of developing a new lidar technique for remote detection of trace amounts of chemical smears on surfaces, particularly for applications to the stand-off detection of explosive materials. Our expectation is that the Raman spectra of interesting materials will have resonance responses as the incident wavelength approaches an electronic excitation at ultraviolet wavelengths. The deep ultraviolet wavelength region is also interesting for another reason. Since most fluorescent emissions occur at wavelengths longer than 280 nm, the fluorescent signature tends not to contaminate the Stokes components of the Raman spectra when the excitation laser wavelength is less than about 260 nm (the width of the full Raman spectrum is less than 25 nm for these excitation energies). In addition to the sensitivity gain from molecular scatter cross-section as one selects shorter wavelengths, the resonance Raman process can increase the sensitivity by several orders of magnitude. As an example of an ultraviolet resonance Raman measurement, Fig. 9 shows the Raman spectrum for a measurement sequence of a liquid benzene sample [22]. In this case, the wavelength of the excitation laser is increased in 0.25 nm steps from 258 to 260 nm. The large change in the Raman spectrum intensity between 750 and 1300 cm^{-1} is apparent as the wavelength of the excitation source increases from 258 to 260 nm. A wide range of materials are currently under investigation for their resonance Raman characteristics. Models of performance for this process are needed to take advantage of the opportunities offered by deep ultraviolet excitation of molecular resonances.

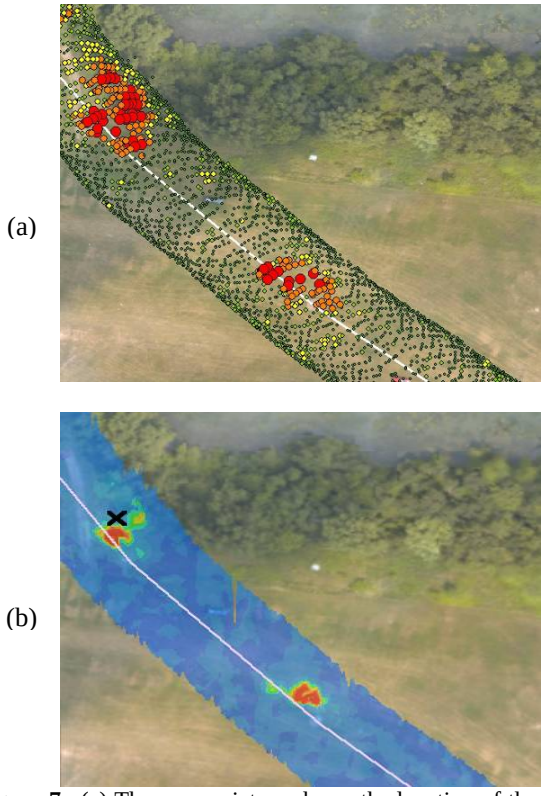

Figure 7. (a) The upper picture shows the location of the laser shots on the surface as the plane flies its course; (b) the locations of high methane concentrations that show leaks in the buried pipeline [17].

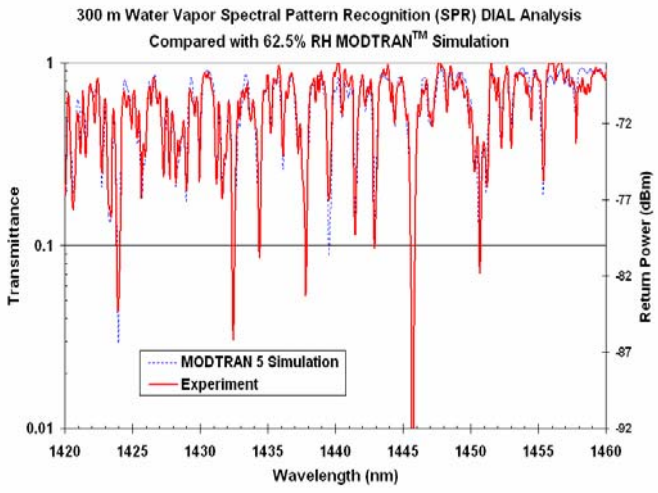

Figure 8. The water vapor spectrum measured using the PSU supercontinuum laser as a lidar transmitter with comparison to the MODTRAN model [20].

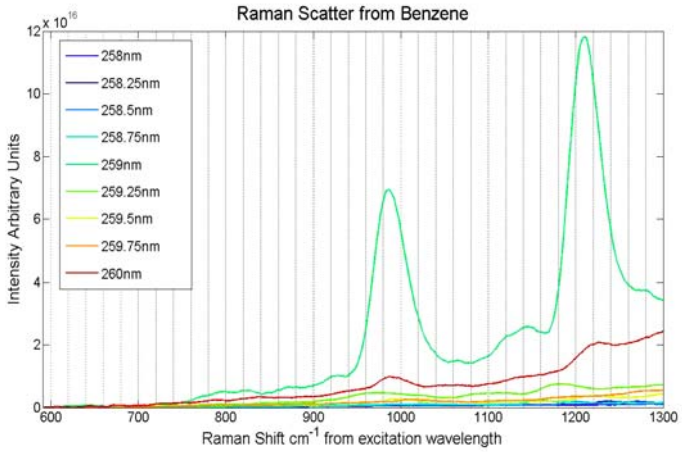

Figure 9. A sequence of Raman spectra obtained by scattering laser wavelengths from 258 to 260 nm in liquid benzene [22].

III. SUMMARY

An improved means for detection and measurement of chemical species at trace concentrations in the atmosphere and on surfaces are a primary focus for several investigations. Many needs exist to meet requirements for detection of explosives and toxic chemicals for DoD and DHS, as well as for air pollution monitoring for state and federal agencies.

Table II lists the several techniques for optical sensors that would be most useful for detection and for measuring the concentration of chemical species. Many factors influence the performance of such sensors, in particular, the transmitted intensity, receiver collection area, detector sensitivity, as well as the instrument operating environment and range to target.

Table II. Primary Methods for Standoff Optical Detection are Listed with Estimates of Sensor Performance

Optical Techniques and Detection Range (Est.)
DIAL ~ ppm
100 ppm – 10 ppb
DAS ~ 10's of ppb
10 ppm – 100 ppt
Raman ~ 100's ppm
1000 ppm – 10 ppm
Raman/DIAL ~ 10 ppb (Hartley band of ozone)
Resonance Raman ~ ppm
100 ppm – 10 ppb - - - - 100 ppt
Fluorescence ~ 10's of ppm
1 ppm – 10 ppt

ACKNOWLEDGEMENTS

The PSU lidar development, testing, and field investigations have been supported by the following organizations: US Navy through SPAWAR PMW-185, NAVOCEANO, NAWC Point Mugu, ONR, DOE, EPA, Pennsylvania DEP, California ARB, NASA and NSF. The hardware and software development has been possible because of the excellent efforts of several engineers, technicians, and graduate students at PSU in the Applied Research Laboratory and the Department of Electrical Engineering. Special appreciation for contributions to these developments goes to D. Sipler, B. Dix, Gil Davidson, D.B. Lysak, T.M. Petach, F. Balsiger, T.D. Stevens, P.A.T. Haris, M. O'Brien, S.T. Esposito, K. Mulik, A. Achey, E. Novitsky, G. Li, Sachin Verghese, and many additional graduate students who have made contributions to these efforts. The NE-OPS research investigations have been supported by the USEPA STAR Grants Program #R826373, Investigations of Factors Determining the Occurrence of Ozone and Fine Particles in Northeastern USA, and by the Pennsylvania DEP. The cooperation and collaborations with many university and government laboratory researchers are gratefully acknowledged, in particular the contributions of Rich Clark, S.T. Rao, George Allen, Bill Ryan, Bruce Doddridge, Steve McDow, Delbert Eatough, Susan Weirman, and Fred Hauptman are particularly acknowledged. Major collaborative efforts with Steve Stearns of ITT and with Charlie Ritchey of Michigan Aerospace Corporation are acknowledged.

REFERENCES

[1] Berk, A., et al., "MODTRAN5: A reformulated atmospheric band model with auxiliary species and practical multiple scattering options," in Algorithms and Technologies for Multispectral, Hyperspectral, and Ultraspectral Imagery X, *Proceedings of SPIE*, v. 425, S. Shen, ed., pp. 341 – 347, 2004.

[2] Inaba, H. and T. Kobayasi, "Laser-Raman Radar," Opto-electronics, 4 101- 123, 1972.

[3] Inaba, H., "Detection of Atoms and Molecules by Raman Scattering and Resonance Fluorescence," in Laser Monitoring of the Atmosphere, (Ed. E.D. Hinkley), Springer-Verlag, 153-236, 1976.

[4] Kobayshi, Takao, "Techniques for Laser Remote Sensing Environment," Remote Sensing Reviews, Vol. 3, pp. 1-56, 1987.

[5] Philbrick, C.R., D.B. Lysak, T.D. Stevens, P.A.T. Haris and Y.-C. Rau,"Atmospheric Measurements Using the LAMP Lidar during the LADIMAS Campaign," 16th International Laser Radar Conference, NASA Pub. 3158, 651-654, 1992.

[6] Rajan, S., T. J. Kane and C. R. Philbrick, "Multiple-wavelength Raman Lidar Measurements of Atmospheric Water Vapor," Geophys. Res. Let. 21, 2499-2502, 1994.

[7] Philbrick, C.R., and K Mulik, "Application of Raman Lidar to Air Quality Measurements," Proceedings of the SPIE Conference on Laser Radar Technology and Applications V, 4035, 22-33, 2001.

[8] Mulik,K.R., and C.R. Philbrick, "Raman Lidar Measurements of Ozone During Pollution Events," in Advances in Laser Remote Sensing, Selected papers from 20th ILRC, July 2000 in Vichy France, pp 443-446, 2001.

[9] Doddridge, Bruce G., Richard D. Clark and C. Russell Philbrick, "Airborne Measurements of Chemistry and Aerosol Optical Properties during NARSTO Northeast Oxidant and Particle Study," Proceedings of the American Meteorological Society 4th Conference on Atmospheric Chemistry, 146-152, 2002.

[10] Philbrick, C. Russell, "Overview of Raman Lidar Techniques for Air Pollution Measurements," in Lidar Remote Sensing for Industry and Environment Monitoring II, SPIE , 136-150, 2002.

[11] Philbrick, C.R., "Raman Lidar Descriptions of Lower Atmosphere Processes," Lidar Remote Sensing in Atmospheric and Earth Sciences, Proc. 21st ILRC, Valcartier, Quebec Canada, 535-545, 2002.

[12] Philbrick, C.R., "Raman Lidar Characterization of the Meteorological, Electromagnetic and Electro-optical Environment," Proc. SPIE Vol. 5887, Lidar Remote Sensing for Environmental Monitoring VI; Upendra N. Singh; Ed., p. 85-99, Aug 2005.

[13] Collier, Paul Jason, "RF Refraction on Atmospheric Paths from Raman Lidar," MS Thesis Penn State University, Department of Electrical Engineering, August 2004.

[14] Willitsford, Adam, C. R. Philbrick, "Lidar Description of the Evaporative Duct in Ocean Environments," Proc. SPIE Vol. 5885, Remote Sensing of the Coastal Oceanic Environment; Robert J. Frouin, Marcel Babin, Shubha Sathyendranath; Eds., p. 140-147, Aug 2005.

[15] Stearns, Steven V., Raymond T. Lines, Christian J. Grund and C. Russell Philbrick, Active Remote Detection of Natural Gas Pipeline Leaks, Technology Status Reports of NETL Department of Energy, web: http://www.netl.doe.gov/scngo/Natural%20Gas/index.html + Projects + Remote Sensing Technologies + Leak Detection + DE-FC26-03NT41877 + Status Assessment

[16] Philbrick, C. Russell, Zhiwen Liu, Hans Hallen, David M. Brown, and Adam Willitsford, “LIDAR Techniques Applied to Remote Detection of Chemical Species in the Atmosphere,” C. Russell Proc ISSSR, 2006 http://www.isssr2006.com/TALK_UPLOADS/Russell-Philbrick.pdf

[17] Murdock, Darryl G., Steven V. Stearns, R. Todd Lines, Dawn Lenz, David M. Brown, and C. Russell Philbrick, “Applications of real-world gas detection: Airborne Natural Gas Emission Lidar (ANGEL) system,” *J. Applied Remote Sensing*, 2, 023518, 18pp (2008).

[18] Alfano, R.R., *Supercontinuum Laser Source*, (Springer Verlag, New York, 1989).

[19] Begnoché, J. "Analytical Techniques for Laser Remote Sensing with a Supercontinuum White Light Laser" The Pennsylvania State University, M.S. Thesis, 2005.

[20] Brown, David M., Kebin Shi, Zhiwen Liu, and C. Russell Philbrick, “Long-path supercontinuum absorption spectroscopy for measurement of atmospheric constituents,” *Optics Express*, 16, 8457-8471 (2008).

[21] Brown, David M., Zhiwen Liu, and C. Russell Philbrick, “Supercontinuum Lidar Applications for Measurements of Atmospheric Constituents,” in *Laser Radar Technology and Applications XIIII*, Proc. SPIE Vol. 6950, 69500B, 11 pp. (2008).

[22] Willitsford, Adam C., Todd Chadwick, Hans Hallen, C. Russell Philbrick, “Resonance Raman Measurements Utilizing a Deep UV Source,” in *Laser Radar Technology and Applications XIIII*, Proc. SPIE Vol. 6950, 69500A, 8 pp. (2008).

This paper was presented a lead invited talk at the
Fourth Symposium on Lidar Atmospheric Applications,
11–15 January 2009, Phoenix, Arizona for the 89th
American Meteorological Society Annual Meeting.